Validation of MODIS-Aqua Aerosol Products C051 and C006 over the Beijing-Tianjin-Hebei Region

Ke Wang, Xuejin Sun *, Yongbo Zhou and Chuanliang Zhang

Institute of Meteorology and Oceanography, National University of Defense Technology, Nanjing 211101, China; tomwang3@outlook.com (K.W.); Yongbo.zhou@yahoo.com (Y.Z.); zhangcl2015@126.com (C.Z.)

* Correspondence:xuejin.sun@outlook.com; Tel.: +86-151-9597-0375

Abstract: The recently released MODerate resolution Imaging Spectroradiometers (MODIS) Collection 6(C006) includes several significant improvements, which are expected to do well in analyzing aerosols and using the observations for air pollution application. The C006 Aerosol Optical Depth (AOD) retrievals should be validated completely before they will be applied to specific research. However, the validation of C006 AOD retrievals at a regional scale is limited. Therefore, this study evaluated the performance of the MODIS-Aqua Collection 51 (C051) and C006 AOD retrievals over the Beijing-Tianjin-Hebei region in China from 2006 to 2015 using ground-based Sun photometers. The algorithms of the AOD product include Dark Target (DT) and Deep Blue (DB). The results indicated that the improvements in DT C006 were slight, as the expected error (EE) increased by almost 9% over the two sites, and the DT C051 and DT C006 AOD were overestimated for both sites. DB C006 presented an improvement over DB C051, and a better correlation was observed between the collocated DB C006 retrievals and Sun photometer data (R ranged from 0.9343–0.9383). There was an increase in the frequency from DT C051 to DT C006, in the range 0.6–1.5, over the two sites; moreover, the AOD from the DB retrievals had a very narrow range (0.1–0.3). The spatial distribution of the AOD values was high (AOD > 0.7) over the southeastern region and low (AOD < 0.3) over the northwestern region. Changes in the DT C006 algorithm resulted in an increased AOD (0.085) for the region. The AOD values in spring and summer were higher than those in fall and winter. By subtracting the C051 AOD from the corresponding C006 values, greater positive changes (~0.2) were found in the southeastern areas during summer, presumably as the updated cloud-masking allowed heavy smoke retrievals. The accuracy of the AOD retrievals depended on the assumptions of surface reflectance and the selection of the aerosol model. The use of the DB C006 algorithm is recommended for the Beijing and Xianghe sites. Because of the limitations of the DT algorithm over sparsely vegetated surfaces, the DT C006 product is recommended for Xianghe.

Keywords: MODIS C006; AERONET; aerosol optical depth (AOD); validation

1. Introduction

Atmospheric aerosols, i.e., small solid and liquid particles suspended in the atmosphere, are one of the most important components of the earth's atmosphere since they play a key role in altering the global energy budget [1], modifying the hydrological cycle [2] and influencing atmospheric visibility [3] and public health [4]. The AErosol RObotic NETwork (AERONET) is a global network of calibrated ground-based Sun photometers. This network provides regular measurements of aerosol optical properties such as aerosol optical depth (AOD) every 15 min [5]; however, limited sites and samples make it challenging to obtain the distribution of AOD, both globally and regionally. In this context, a series of satellite sensors have been deployed for characterizing the global distribution of aerosols [6–11]. Compared with ground-based AOD data, the satellite-derived AOD has lower accuracy. Therefore, it is essential to validate the satellite-derived AOD against ground-based AOD data.

The MODerate resolution Imaging Spectroradiometer (MODIS) instrument aboard the Terra and Aqua satellites has provided nearly global observations on a daily basis since 2000 and 2002, respectively, thanks to its wide swath (~2330 km). As a passive sensor, MODIS measures sun-reflected and emitted long-wave radiation across 36 channels (spanning the range from 0.41 to 14.5 μm) at various spatial resolutions (250 m, 500 m and 1 km). Aerosol observations by MODIS are made at 7 wavelengths, from near-UV to the mid-VIS spectrum, through the implementation of retrieval algorithms, the concept of which varies among the different surface types (land, ocean and arid areas) [12]. Although the MODIS aerosol retrieval algorithm has been continuously operated and upgraded, the principle of the algorithm is based on the Dark Target approach, which was introduced by Kaufman et al. [13]. Validation must be conducted before AOD retrievals can be used for multiple purposes, such as radiation budget calculations, climate change modeling and air quality assessments. Surface-based measurements, particularly those derived from AERONET, are considered as truth and are used to validate the satellite products [5,14–16].

MODIS AOD products have undergone five upgrades since the launch of Terra [12]. The last major update of the dark-target aerosol products was labeled Collection 5 (C005 for Terra and Collection 51 or C051 for Aqua). Details of the major changes with respect to the previous changes (Collection 4, C004) are presented in the literature [9,15]. Global validation results of collocated Collection 5/51 AOD retrievals against high quality AERONET AOD showed better agreement over land than C004. An evaluation of C005 and C004 AOD at 550 nm against ground–based measurements over the Mediterranean basin was performed [17], and C005 data were better correlated with the corresponding 29 AERONET sites. Levy et al. [15] performed a comprehensive assessment of MODIS C005 AOD retrievals versus quality assured AERONET-derived products across 300 sites. In addition, Li et al. [18] evaluated C005 using AERONET datasets from 13 sites across China.

The recent Collection 6 (C006) was released in 2014. Compared with the former C005, several modest improvements in the cloud-masking, gas and Rayleigh correction, surface reflectance assumption and quality assurance were included [12]. Some enlightening results on the evaluation of the C006 AOD products have been reported. For example, Levy et al. [12] comprehensively introduced the C006 algorithm for aerosol retrieval and compared C006 and C051 AOD using ground-based Sun photometer data; the preliminary results indicated that C006 AOD retrievals are at least as good as C051 AOD retrievals. Floutsi et al. [19] validated the reliability of e MODIS-Aqua AOD over 13 years and found an improvement from C005 to C006. Bilal et al. [20] validated C051 and C006 AOD against AERONET measurements over Pakistan and recommended the use of DT C006 AOD for Karachi as a result of its higher accuracy and fewer uncertainties compared with C051 AOD.

The Beijing-Tianjin-Hebei region, especially the Chinese capital, Beijing, is subjected to severe haze as a result of pollutant emissions and local weather conditions during winter [21]. Serious air pollution over the Beijing-Tianjin-Hebei region has attracted considerable attention from society. Therefore, numerous studies based on satellite data have been conducted to examine the spatiotemporal behavior of aerosols over the region [22–24]. It is worth noting that the new collection of AOD products should be completely validated before they are applied to regional air quality research. The previous AOD retrieval collections have been widely validated, but the validation of C006 over the Beijing-Tianjin-Hebei remains limited [25,26].

The key objective of this study is to evaluate the performance of the MODIS-Aqua DT and DB Level 2 AOD retrievals derived from Collections 051 and 006, over the period 2006–2015. Toward this aim, the AERONET AOD records from the Beijing and Xianghe stations, located in the Beijing-Tianjin-Hebei region, have been used as reference data. Comprehensive and in-depth evaluations were performed in this paper, and the applicability and retrieval accuracy were determined over the region.

2. Experiments

2.1. Study Area

The Beijing-Tianjin-Hebei region is an important capital economic circle in China. Hebei Province is the main body, and Beijing, the capital of China, is in the middle of the Province. The eastern region adjacent to the Bohai Gulf is Tianjin. The terrain of this area slopes downwards from the northwest to the southeast, and the geographic types are various and complicated. Due to the specific terrain and densely populated land area, Beijing has suffered from severe air pollution in recent years. AERONET level 2.0 data from two sites, Beijing and Xianghe, were obtained for this paper. As shown in Figure 1, the Xianghe site (116.962° E, 39.754° N) is located in a suburb of Tianjin approximately 80 kilometers east of the Beijing site (116.381° E, 39.977° N).
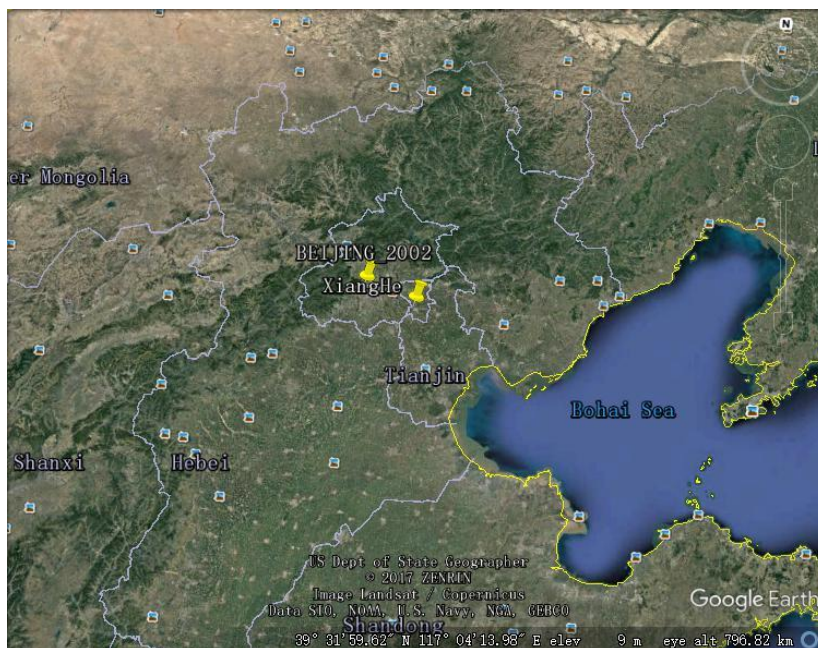
Figure 1. Locations of the two AERONET sites over the Beijing-Tianjin-Hebei region (the yellow pointers represents the two sites, Beijing and Xianghe).

2.2. AERONET

AERONET is a worldwide ground-based aerosol observation network of approximately 700 well-calibrated CIMEL Sun photometers, which operate continuously and provide AOD measurements over a wide spectral range with low uncertainty (three to five times higher accuracy than satellite-based observation) [5,9]. Three levels of AOD products are included: Level 1.0, Level 1.5 and Level 2.0 (Available online: http://aeronet.gsfc.nasa.gov) [20]. Level 2.0 AOD products are cloud screened and quality assured. More than 20 sites are located in China, although most of them provide datasets shorter than 5 years. The CIMEL Sun photometers at Beijing and Xianghe have provided more than ten years of AOD data since 2002, and these data act as a reference for the evaluation of the C051 and C006 MODIS AOD retrievals.

Since AERONET AOD does not include the 550 nm channel, 440 nm and 675 nm AOD data are interpolated to 550 nm according to the following two equations based on the Angström exponent (α) [9]

$$\tau_\lambda = \beta\lambda^{-\alpha} \tag{1}$$

$$\tau_{0.55} = \tau_{0.50}(0.50/0.55)^{\alpha_{440-675}} \tag{2}$$

2.3. MODIS Data

The MODIS Level 2 aerosol products were generated from the MODIS Level-1 and Atmosphere Archive and Distribution System (Available online: http://ladsweb.nascom.nasa.gov) [12]. AOD retrievals from C051 and C006 are based on the DT and DB algorithms and provide global AOD observations at a nominal resolution of 10 km with a relatively high temporal resolution of 1–2 days [27]. Because the DT algorithm cannot retrieve AOD over bright surfaces, Hsu et al. introduced the DB algorithm in Collection 5, only over bright surfaces [28]. The enhanced generation DB algorithm in Collection 6 is able to retrieve AOD all bright and dark surfaces except for cloud mask and snow/ice surfaces. Details of the enhanced DB algorithms have been reported in Hsu et al. [29].

Products for MODIS-Terra and MODIS-Aqua are known as MOD04 and MYD04, respectively. Compared with MODIS-Terra, MODIS-Aqua has small calibration changes; thus, MODIS-Aqua products were obtained [30]. In this study, MODIS-Aqua AOD retrievals were obtained (Table 1), and only the highest quality products (QAC = 3) were analyzed (Table 2) [12].

Table 1. Quality assurance (QA) flags of the MODIS C051 and C006 AOD product.

Scientific Data Set (SDS) Name	Long_Name
Optical_Depth_Land_And_Ocean	Collection 5: Land QAC = 3; Ocean QAC = 3 (best)
	Collection 6: Land QAC = 3; Ocean QAC $\geq$ 1 (average)
Deep_Blue_Aerosol_Optical_Depth_550_Land	Land QAC = 1,2,3

Table 2. Quality assurance (QA) flags of the MODIS AOD product.

QA Flags	QA Confidence
0	Bad or No Confidence
1	Marginal
2	Good
3	Very Good

3. Data Processing

Ichoku et al. [31] proposed the temporal and spatial matching method at a global scale. Those authors analyzed aerosol tracks from daily sequences of TOMS image and proposed that the average speed of the aerosol front was 50 km/h. However, the matching scale was not suitable for a regional analysis. Based on the monthly average wind speed of the Beijing-Tianjin-Hebei region from 1971 to 2000, supplied by the China Meteorological Data Sharing Service System (CMDSSS), the two sites show limited differences in wind speed, which is approximately 2–5 m/s (7.2–18 km/h) annually. We assumed that the aerosol front movement speed approaches the horizontal wind speed. Here, we used the modified collocation protocol proposed by Petrenko et al. [32], where the sampling spatial radius is $\pm$25 km. In order to increase the number of collocations, the temporal interval is increased to 60 min.

A series of statistical methods were employed to reveal the algorithm uncertainties. The measurement accuracy of AOD over land was verified as 0.04 or 10% by Mishchenko et al. [33]. As shown in Hansen et al. [34], a minimum AOD of 0.7 is necessary for the accuracy of the retrieval over desert and semiarid areas. Therefore, we should consider the measurement accuracy of the MODIS AOD retrievals (QAC = 3) before the MODIS retrieval accuracy are evaluated. Deming regression was used to estimate the slope and intercept. Additionally, the expected error (EE) was used to evaluate the fraction falling within the EE envelope. The EE of the DT algorithm was calculated by Equation (3) [12] over land and for the EE of the DB algorithm, Equation (4) [12] was recommended. The fraction falling within the EE could partly measure the quality of the retrieval. The relative mean bias (RMB, Equation (5)) shows the retrieval estimation with an RMB of greater than 1 and less than

1, which indicates the respective average overestimation and underestimation of the retrievals. The root-mean-square error (RMSE, Equation (6)) and the mean absolute error (MAE, Equation (7)) are also used for evaluation, and smaller RMSE and MAE values indicate a better performance of the retrievals.

$$EE = \pm(0.05 + 0.15AOD_{AERONET}) \tag{3}$$

$$EE = \pm(0.05 + 0.20AOD_{AERONET}) \tag{4}$$

$$RMB = \left(\overline{AOD_{MODIS}} / \overline{AOD_{AERONET}}\right) \tag{5}$$

$$RMSE = \sqrt{\frac{1}{n}\sum_{i=1}^{n}\left(AOD_{MODIS_i} - AOD_{AERONET_i}\right)^2} \tag{6}$$

$$MAE = \frac{1}{n}\sum_{i=1}^{n}\left|AOD_{MODIS_i} - AOD_{AERONET_i}\right| \tag{7}$$

4. Results and Discussion

Table 3 presents the matching samples of the MODIS AOD retrievals and AERONET AOD at 550 nm for the Beijing and Xianghe AERONET Sun photometers sites. A total of 571 collocations were obtained for DT C051, which is higher than that of DT C006 (N = 493), over Beijing from 2006 to 2015. The collocations for DT C051 and DT C006 over Xianghe were 1012 and 722, respectively. For DB, the collocations for DB C051 were 614 for the Beijing site, i.e., fewer than that of DB C006 (N = 1208). At the Xianghe site, the number of collocations was 127 for DB C051 and 1328 for DB C006. Significant differences were observed between the DB C051 and DB C006 collocations because of their distinct algorithms used in the retrieval process. An obvious change from DB C051 to DB C006 was that the C051 algorithm only retrieves AOD over bright surfaces, whereas C006 can retrieve AOD over both dark and bright surfaces except for cloud mask and snow/ice-covered surfaces [29].

Table 3. Number of MODIS and AERONET AOD values from temporal-spatial matching.

Numbers	Time (Year)										
Site	2006	2007	2008	2009	2010	2011	2012	2013	2014	2015	Total
DTC051-Beijing	61	74	24	74	70	36	41	71	61	59	571
DTC006-Beijing	51	63	17	67	63	30	37	60	49	56	493
DTC051-Xianghe	108	115	76	118	83	108	100	118	120	66	1012
DTC006-Xianghe	75	85	52	84	60	67	72	88	96	43	722
DBC051-Beijing	78	67	42	61	59	69	58	56	68	56	614
DBC006-Beijing	136	132	64	140	133	136	96	128	136	107	1208
DBC051-Xianghe	24	20	11	16	7	9	10	10	10	10	127
DBC006-Xianghe	140	152	110	142	124	150	128	147	147	88	1328

4.1. Evaluation of DT C051 and DT C006 over the Beijing and Xianghe Sites

Figure 2 describes the scatterplots between the two collections (C051 and C006) of MODIS DT AOD values at 550 nm against the corresponding AERONET retrievals for the two sites (Beijing and Xianghe) considered in our evaluation analysis. The AOD bin was set to <0.5 during low aerosol loadings, and bins of 0.5 < AOD < 1, AOD > 1 represent moderate and high aerosol loadings, respectively. Large parts of retrievals exceeded the upper bound of the EE; thus, the DT C051 AOD was greatly overestimated over the two sites because of the underestimation of surface reflectance and single scattering albedo (SSA) of aerosols [35]. As shown in Table 4, the mean overestimations were 51.3% for the Beijing AOD and 18.9% for the Xianghe AOD, which resulted in a larger slope (1.2541–1.2614) for DT C051. Similar results for aerosols over urban bright surfaces have been reported [25]. Although DT C051 presented a stronger correlation with Beijing ground-based observations, DT C006 appeared to improve the quality of retrievals and had low RMSE and MAE values; therefore, collocated DT C006 retrievals were better correlated with the AERONET AOD than those of DT C051 for the high AOD values

over the Beijing site. The fractions within the EE increased from 24.87% to 32.45% and from 68.08% to 77.98% for the Beijing and Xianghe sites, respectively. The DT C006 retrievals were 8–10% less overestimated on average and showed 3% lower uncertainty than the DT C051 retrievals. The results are in agreement with Bilal et al. [25]. However, the AOD over the two sites was still overestimated, with an average overestimation of 10.52–41.64% (RMB ranges from 1.1052–1.4164). The overestimation of DT retrievals is higher than the threshold science requirement indicated by Mishchenko et al. [33]. Overall, the improvements in DT C006 were not evident because the EE increased by almost 9% over two sites. As previous studies reported [15,20,25,35], the findings indicated that underestimation of the precalculated surface reflectance and the use of improper aerosol models in look up tables (LUTs) caused uncertainties.
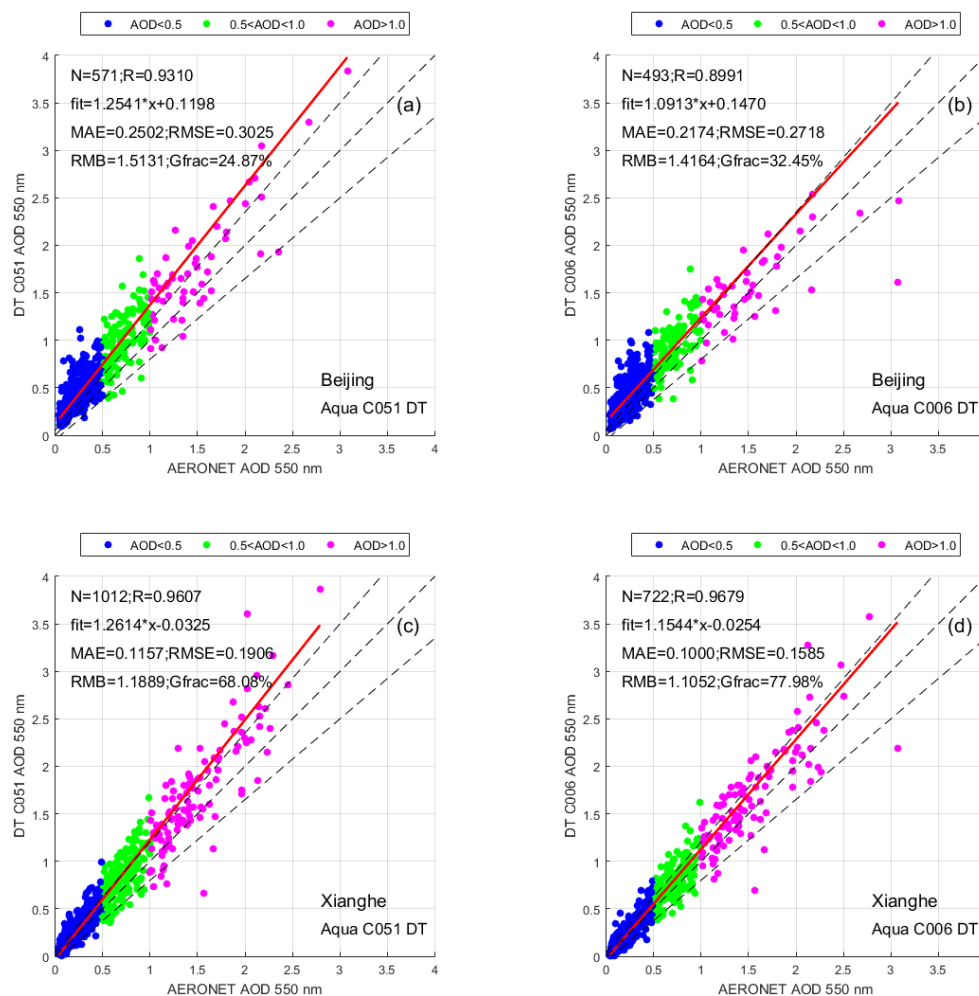

Figure 2. Scatterplots between the two collections (C051 and C006) of MODIS DT AODs at 550 nm against the corresponding AERONET retrievals for the two sites (Beijing (**a**,**b**) and (**c**,**d**) Xianghe) (The red line is the regression line, and the black dashed lines define the envelope of EE; AOD < 0.5: low aerosol loadings; 0.5 < AOD < 1.0: moderate aerosol loadings; AOD > 1.0: high aerosol loadings).

A "good fraction" was defined when more than 66% of the retrievals fell within the EE [12]. DT C051 and DT C006 AOD retrievals over Xianghe achieved this goal. Due to the limitation of the DT algorithm over bright surfaces, the number of collocations over the Xianghe site was almost 1.5–1.8 times higher than that over the Beijing site. Beijing, a typical urban site, is influenced by anthropogenic aerosols and coarse particulates, which result in difficulty in measuring optical properties, and the Sun photometer is surrounded by built-up areas and bare land [23]. Xianghe is a traditional suburban area, dominated by sparse buildings and agricultural land [18]. The surface

reflectance assumptions and the aerosol model in the DT algorithm are better suited to Xianghe than Beijing. The DT AOD retrievals exhibit poor performance over bright surfaces, such as urban and semiarid regions. Therefore, the performance of the MODIS DT algorithm is better for Xianghe in comparison to the Beijing area.

Table 4. Evaluation metrics derived from the scatterplots between MODIS-Aqua and AERONET AOD_{550nm} retrievals. The results are reported separately for each site (Beijing, Xianghe), retrieval algorithm (DT and DB) and collection (C051 and C006).

Site	N [a]	R [b]	Slope	Intercept	Mean [c]	St Dev [d]	RMSE	MAE	RMB	Within EE (%)
DT-Beijing collocations (10 km)										
AERONET	571	0.9310	1.2541	0.1198	0.4626	0.4286				
DT C051					0.6999	0.5028	0.3025	0.2502	1.5131	24.87
AERONET	493	0.8991	1.0913	0.1470	0.4522	0.4387				
DT C006					0.6405	0.4346	0.2718	0.2174	1.4164	32.45
DT-Xianghe collocations (10 km)										
AERONET	1012	0.9607	1.2614	−0.0325	0.4479	0.4539				
DT C051					0.5326	0.5515	0.1906	0.1157	1.1889	68.08
AERONET	722	0.9679	1.1544	−0.0254	0.5162	0.5071				
DT C006					0.5705	0.5679	0.1585	0.1000	1.1052	77.98
DB-Beijing collocations (10 km)										
AERONET	614	0.8833	1.5069	−0.2371	0.5450	0.4949				
DB C051					0.5842	0.6626	0.3257	0.2059	1.0719	51.47
AERONET	1208	0.9343	1.0444	−0.0297	0.4232	0.4593				
DB C006					0.4123	0.4510	0.1655	0.0899	0.9741	81.95
DB-Xianghe collocations (10 km)										
AERONET	127	0.8420	1.8435	−0.5015	0.7062	0.4705				
DB C051					0.8003	0.7347	0.4318	0.2787	1.1333	47.24
AERONET	1328	0.9383	1.1454	−0.0267	0.5060	0.5522				
DB C006					0.5529	0.5964	0.2115	0.1173	1.0926	77.64

N [a]: Total collocations of MODIS AOD retrievals and AERONET AOD (aerosol optical depth); R [b]: The correlation between MODIS AOD retrievals and AERONET AOD values; Mean [c]: The average of MODIS AOD retrievals and AERONET AOD values; St Dev [d]: The standard deviation of MODIS AOD retrievals and AERONET AOD values at 550 nm.

4.2. Evaluation of DB C051 and DB C006 over the Beijing and Xianghe Sites

Figure 3 depicts the scatterplots between the two collections (C051 and C006) of MODIS DB AOD values at 550 nm against the corresponding AERONET retrievals for the Beijing and Xianghe sites. The numbers of collocated DB C006 AOD retrievals (Beijing = 1208 and Xianghe = 1328) are almost 2 and 10 times those for C051 (Beijing = 614 and Xianghe = 127). A previous study also reported collocated DB C006 AOD retrievals were near 2.5 times those for C051 over Beijing_RADI and Beijing_CAMS sites for the year 2012–2013, as DB C006 are suitable for all bright and dark surfaces, except for cloud-masking and snow/ice-covered land [22]. The MODIS DB C051 AOD was underestimated during low aerosol loadings and overestimated during high aerosol loadings, which led to large slopes (1.5069–1.8435) and large negative intercepts (0.2371–0.5015). As Sayer et al. [36] noted, a large slope is caused by an unsuitable aerosol model and the large magnitude of intercept can be attributed to errors in the surface reflectance estimation. DB C051 exhibited poor performance over the two sites, and it failed to reach an EE of 66%, with a value of 51.47% for Beijing and 47.24% for Xianghe. The enhanced DB algorithm improved the quality of the AOD retrievals, and a better correlation was observed between the collocated DB C006 retrievals and AERONET (R ranged from 0.9343–0.9383) (Figure 3b,d). In agreement with Bilal et al. [25], the DB C006 retrievals had 1.97–2.0 times smaller RMSE values, and

2.29–2.38 times lower MAE. On clear days, the DB C006 algorithm appeared to improve the accuracy of the surface reflectance estimation and reduced the magnitude of the intercepts because of the dynamic surface database applied in the DB C006 algorithm [29,35].
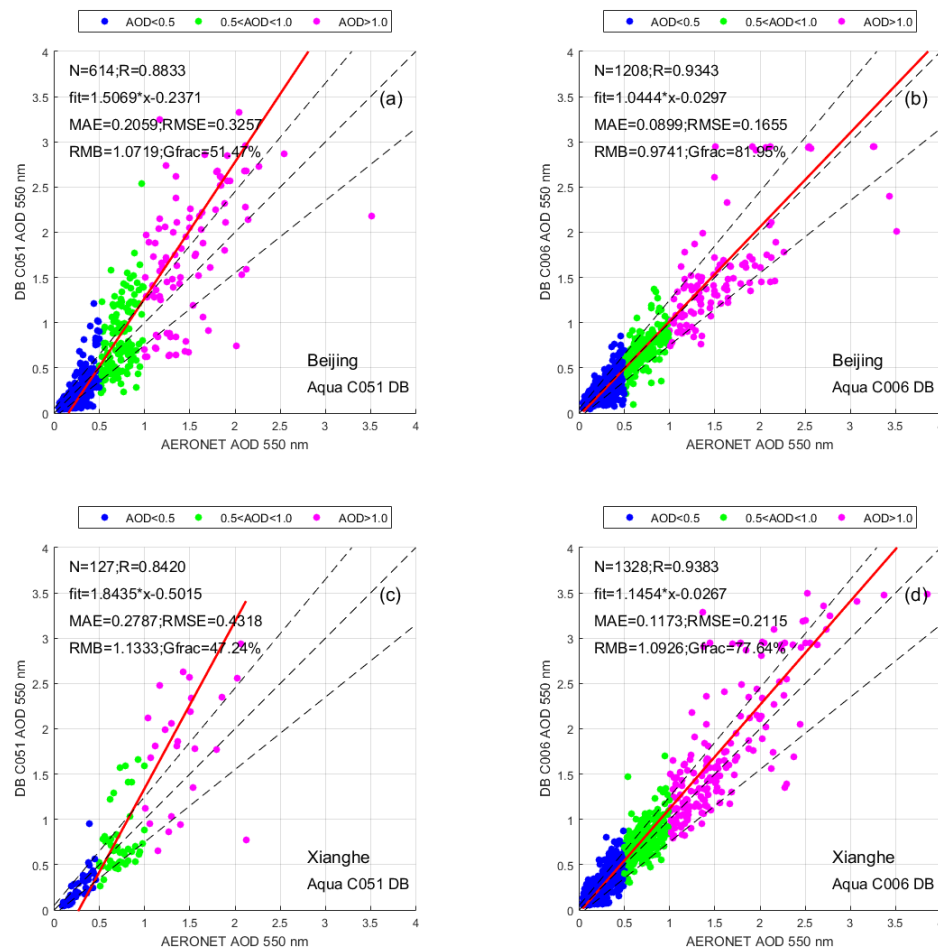

Figure 3. Scatterplots between the two collections (C051 and C006) of MODIS DB AODs at 550 nm against the corresponding AERONET retrievals for the two sites (Beijing (**a**,**b**) and Xianghe (**c**,**d**)) (The red line is the regression line, and the black dashed lines define the envelope of EE; AOD < 0.5: low aerosol loadings; 0.5 < AOD < 1.0: moderate aerosol loadings; AOD > 1.0: high aerosol loadings).

The DB C006 AOD retrievals over the two sites were well correlated with the ground-based observations, and the DB C006 AOD values over Beijing outperformed those over Xianghe. With higher EE and smaller uncertainties, DB C006 AOD over the Beijing site produced minor underestimates (RMB = 0.9741). The regression line of DB C006 for the Beijing site tended to approach the one-to-one line. However, the DB C006 still showed an overestimation for high AOD over Xianghe.

In general, the radiance measured by satellite is derived from interactions of surface, aerosols, atmospheric molecules; thus, it is a mixed signal [37]. However, separating aerosol information from mixed information is difficult. Overall, the quality of the retrieval depends on the accuracy of the surface reflectance and the aerosol model. Distinguishing the aerosol contribution from a mixed signal during low aerosol loading is difficult because of the relatively larger surface reflectance. During high aerosol loading, the inaccuracy of the aerosol model in LUT leads to obvious uncertainties and errors. In the following Section 4.3, the mean geographical distribution of the 10-year average AOD and the absolute differences between the two collections of DT and DB retrievals are discussed. Then, Section 4.4 presents the analysis for the seasonal geographical distributions between the two collections of DT retrievals and their differences.

4.3. Spatial Variability of MODIS-Aqua DT and DB AOD Retrievals

Figure 4 shows the spatial distribution of the multiyear-averaged C051 and C006 AOD over the Beijing-Tianjin-Hebei region. In order to highlight the differences between the two collections, we adopted the protocol that aggregated the map with a 15-km grid without regarding the minimum number of retrievals [37]. Apart from some details, the two collections of DT retrievals indicated similar spatial distribution patterns and varied in aerosol loading with multiyear averaged AOD of 0.5042 for DT C006 and 0.4957 for DT C051. As shown in Figure 4a,b, AOD values were high over the southeastern region and low over the northwestern region. Beijing, Tianjin and the south of Hebei exhibited higher AOD (>0.7) values, whereas lower AOD (<0.3) values occurred in the northwestern region, i.e., the Yanshan Mountains [24,38]. From Figure 4c, areas with obvious positive changes (~0.1) were also found in the southwestern region, especially the cities Baoding and Shijiazhuang. Small positive (~0.05) changes were located in the remaining regions except the northwestern areas. The mean value of the spatial difference (C006-C051) was 0.0085, which was smaller than the global results (0.01) over land [12]. There were negative changes (~0.05) centered in Beijing from DT C051 to DT C006. As described in Section 4.1, the modest improvements in DT C006 retrievals accounted for the results. In Figure 4c, the DB C051 AOD retrievals had more pixels with no data compared with DB C006. The DB C006 retrievals exhibited similar distribution patterns as the DB C051 retrievals AOD over the valid pixels, but they varied in aerosol loading. The mean value of DB C006 AOD over the region was 0.3824 lower than the DT retrievals. Furthermore, the DB algorithms appeared to underestimate AOD at the Beijing site (RMB = 0.9741), stated in Section 4.2. The unusual differences in coastal regions indicated that the 250-m resolution water mask method should be modified [12].
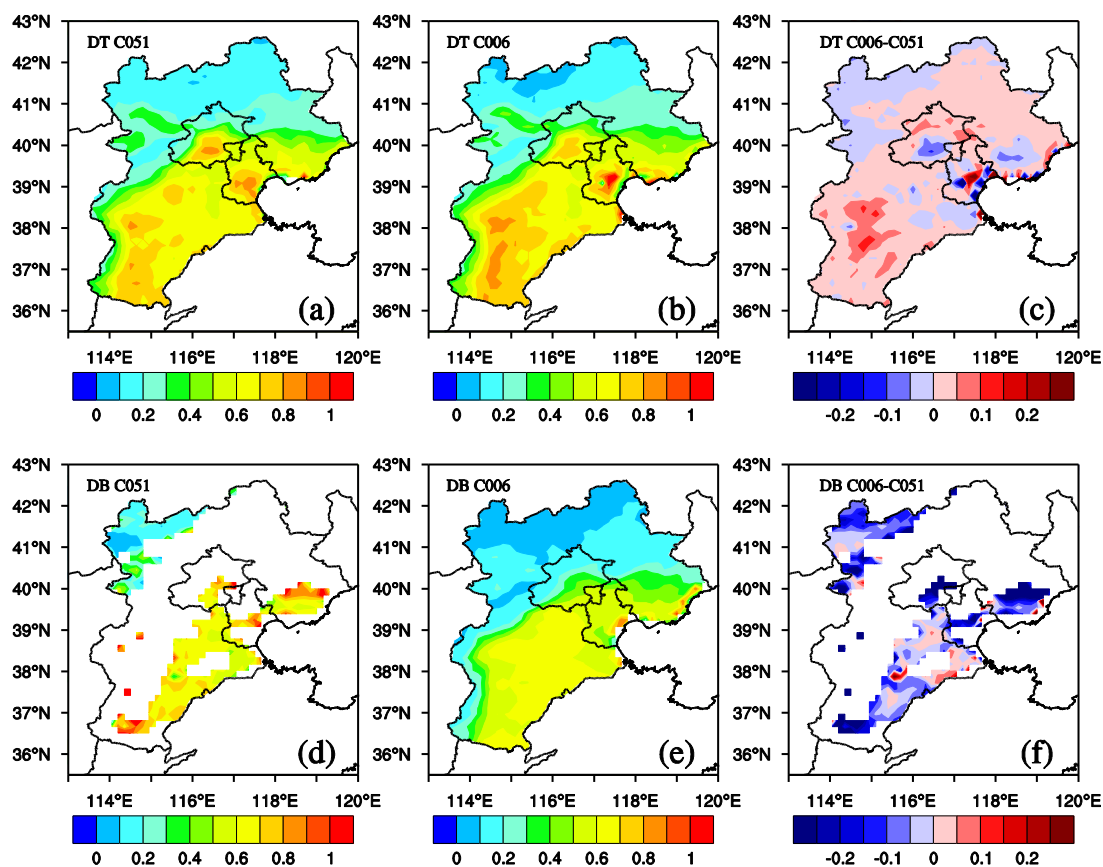

Figure 4. Mean geographical distribution, representative for the period 2006–2015, of the MODIS-Aqua DT (**a**,**b**) and DB (**d**,**e**) AOD_{550nm} values (QAC = 3), over the Beijing-Tianjin-Hebei region. The absolute differences (C006-C051) for the DT (**c**) and DB (**f**) retrieval algorithms are also provided.

　　　Figure 5 depicts the spatial distribution of the multiyear-averaged collocated C051 and C006 retrievals for the DT and DB algorithms over the Beijing-Tianjin-Hebei region. In Figure 5a, compared with DT C051 and DT C006 AOD, the collocated DT retrieval results showed the same spatial distribution patterns. The DT C006 AOD value was much higher in Tianjin, with the highest value exceeding 1.1 in comparison with DT C051 and the collocated retrievals over the southeastern areas. Of course, the collocated DB AOD result indicated exactly the same patterns as the distribution of DB C006, i.e., applicability across the entire landscape.
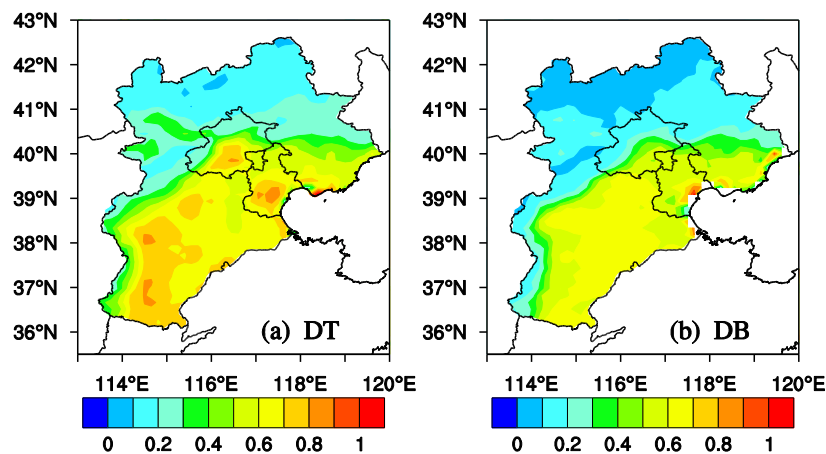
Figure 5. Mean geographical distribution, representative of the period 2006–2015, of the MODIS-Aqua collocated C051 and C006 retrievals DT (**a**) and DB (**b**) AOD_{550nm} values (QAC = 3), over the Beijing-Tianjin-Hebei region.

　　　Plotted in Figure 6 are the frequency histograms of the MODIS-Aqua DT and DB AOD_{550nm} (QAC = 3) for both C051 and C006. In order to construct these histograms, we utilized the method proposed by Remer et al. [39] to accumulate the retrieval boxes. In Figure 6a, a wide distribution AOD was found at the Beijing site with an average AOD of 0.83 for DT C051 and 0.79 for DT C006. There was an increased frequency from DT C051 to DT C006 in the range of 0.6–1.5 over the two sites in Figure 6a,b. In particular, it is worth mentioning the increase in high AOD frequency in Levy et al. [12]. Moreover, the distribution from the two collections of DT was unimodal at the Xianghe site and the peak values are near 0.15 in Figure 6b. Additionally, the distribution of the DT retrievals was distinct from the DB retrievals at the two sites. As shown in Figure 6c,d, an evident increase in the range of 0.1–0.3 from the DB C051 to the DB C006 retrievals was noted. For example, the AOD from DB retrievals had a very narrow range (0.1–0.3), with 44% of AOD retrievals for DB C051 and 64% for those of DB C006 falling within the range at the Beijing site.
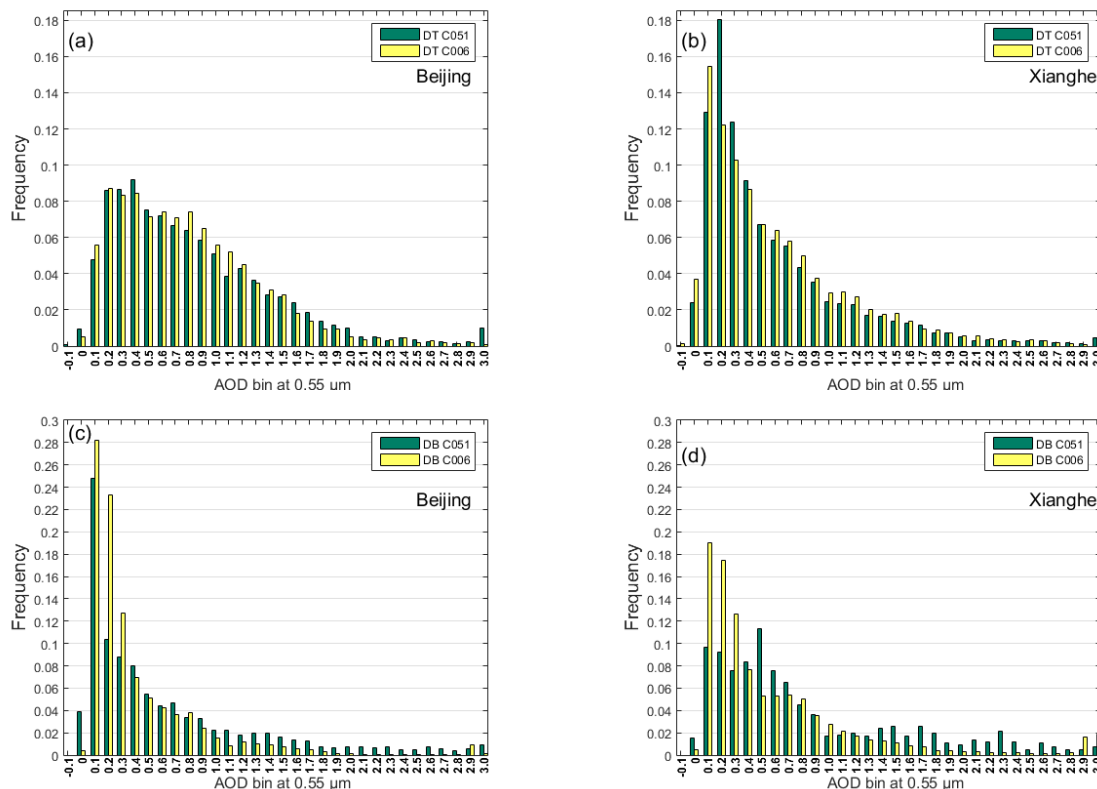
Figure 6. Frequency histograms of the MODIS-Aqua DT (**a**,**b**) and DB (**c**,**d**) AOD$_{550nm}$(QAC = 3) for both C051 (Green) and C006 (Yellow) over the 25-km sampling space centered on the two sites (Beijing and Xianghe) for the period 2006–2015.

4.4. Seasonal Spatial Distribution of MODIS DT C051 and DT C006

Figure 7 shows the seasonal geographical distribution of MODIS DT C051 and DT C006 and their differences (C006-C051). We used the method in Liu et al. [40] and Sun et al. [24] to divide the four seasons. The geographical distribution of MODIS DT AOD in four seasons showed similar patterns with multi-year average spatial distribution described in Section 4.3. The AOD showed evident seasonal variation from the first two columns of Figure 7, which exhibited AOD values that were higher in spring and summer and lower in autumn and winter [24]. As shown in Figure 7d,e, summer had the highest AOD (0.6605 for C006 and 0.6147 for C051) because the increase in temperature and humidity increased the condensation nuclei over the Beijing-Tianjin-Hebei region [24,41]. Furthermore, this region frequently suffers from severe sand dust weather in spring, which increases the AOD. In fall and winter, rainfall and snowfall reduce the particulates suspended in the air and decrease the AOD.

Greater positive deviations (~0.2) between the collections of DT retrievals were manifested in the southern region during summer, where the primary sources of aerosols are heavy smoke emitted from steel factories. Similar large absolute changes over southeastern Asia and Canada in July were reported by Levy et al. [12], presumably as upgrades of the cloud mask in DT C006 allows for heavy smoke retrievals. As stated in Section 4.1, DT C006 reduced the overestimations over the Beijing and Xianghe sites. From the third column of Figure 6, the central region, Beijing, always showed negative changes (~0.15) during all seasons. The results can be attributed to adjusted aerosol type as a function of season and location [12]. The seasonal geographical distribution of collocated DT retrievals revealed minor changes near the Bohai Gulf during spring and summer in Figure 8. Evident changes in land/sea cover may account for the missing pixels [12].
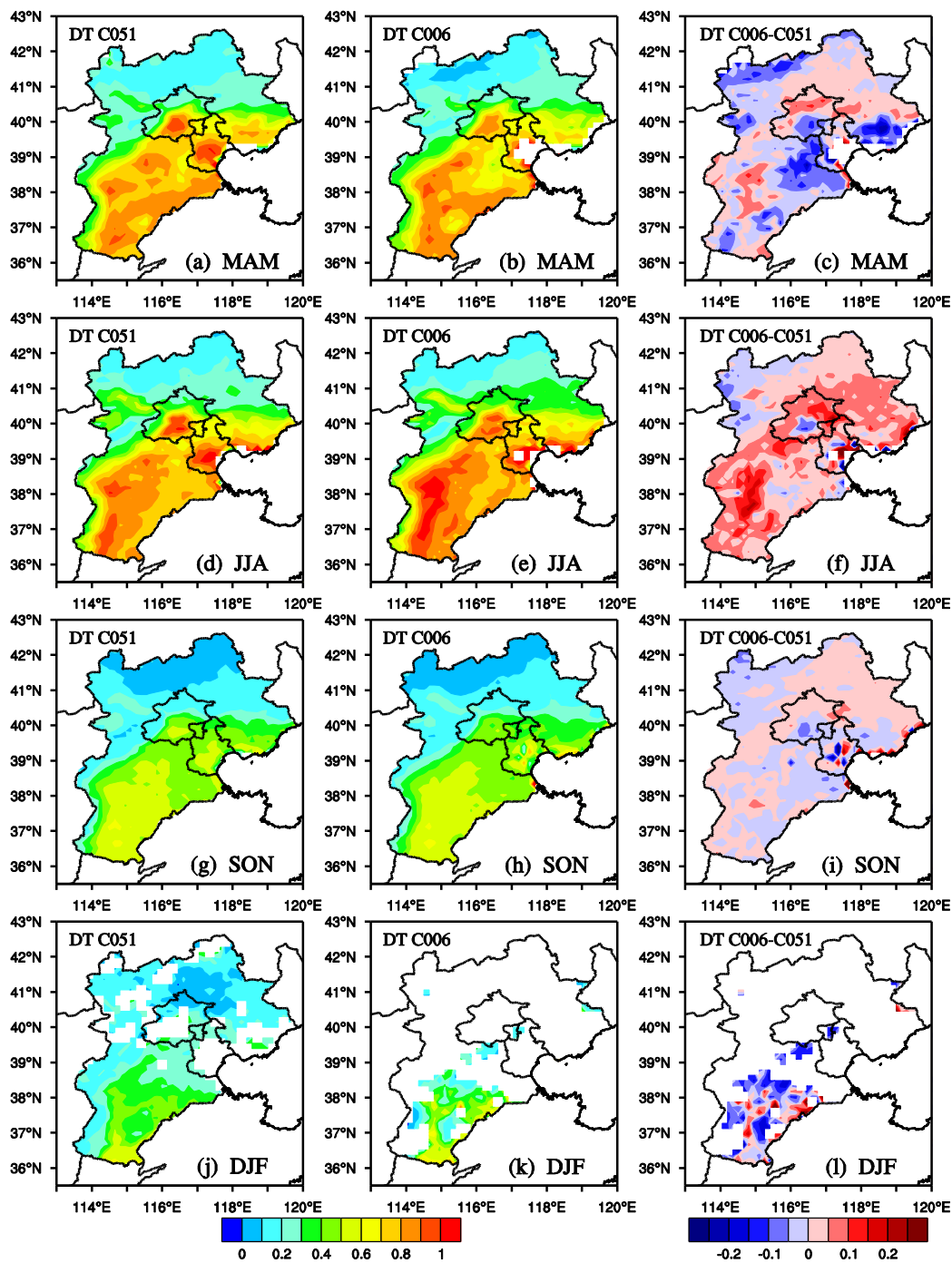
Figure 7. Seasonal geographical distributions of MODIS-Aqua DT AOD$_{550nm}$ retrievals for the period 2006–2015 over the Beijing-Tianjin-Hebei region. For each row, the left panel is the retrieval results from DT C051, the middle panel is from DT C006, and the right panel is the absolute differences (C006-C051). (In the letters from (**a**) to (**l**): December–January–February (DJF), March-April-May (MAM), June–July–August (JJA), and September–October–November (SON)).
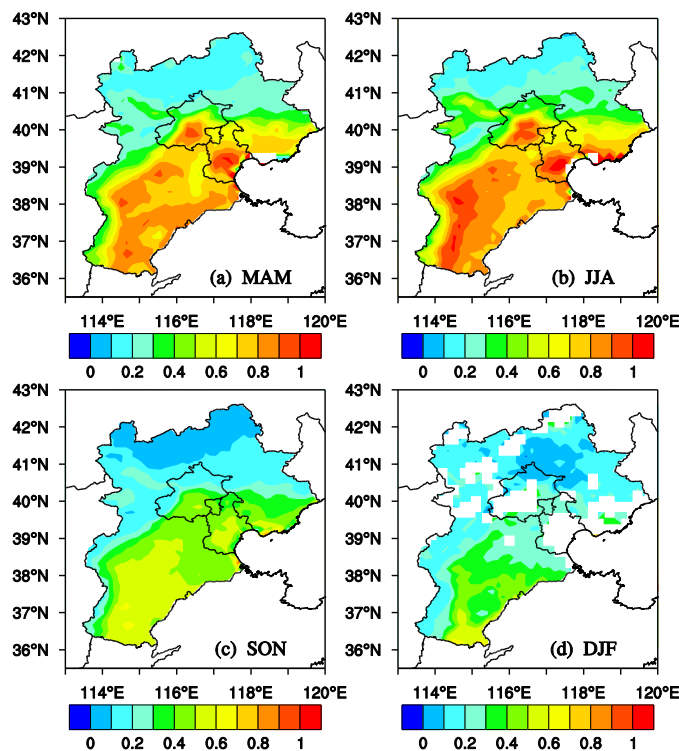
Figure 8. Seasonal geographical distributions of MODIS-Aqua collocated DT AOD$_{550nm}$ retrievals for the period 2006–2015 over the Beijing-Tianjin-Hebei region. The letters from (**a**) to (**d**) represent spring, summer, fall and winter in turn.

5. Conclusions

Although the recently released MODIS Collection 6 AOD retrievals have been evaluated at the global scale, evaluations at a regional level are limited. In this paper, we evaluated the performance of the MODIS-Aqua Level 2 C051 and C006 AOD retrievals over the Beijing-Tianjin-Hebei region for the period 2006–2015. The AOD retrievals based on the DT and DB algorithms were validated using ten years of AERONET data from the Beijing and Xianghe sites.

The results showed that both DT C051 and DT C006 AOD values were overestimated over the two sites. The systematic overestimations were caused by the underestimation of surface reflectance and aerosol single albedo. The improvements in DT C006 were slight because the EE increased by almost 9% over the two sites. The results indicate that the DT C006 algorithm is more suitable for Xianghe than for the Beijing site because of the widespread dense vegetation over Xianghe.

DB C051 AOD retrievals were underestimated for low AOD values and overestimated for high AOD. Enhanced DB algorithm (C006) AOD retrievals performed better than those of DB C051, as the DB C006 retrievals had 1.97–2.0 times smaller RMSE, and 2.29–2.38 times lower MAE than DB C051. The sampling frequency strongly increased because the applicability of the DB C006 algorithm is across entire landscapes. The numbers of collocated DB C006 retrievals were higher than those for DT C006 because of the heavy aerosol loading and the limitations of the DT algorithm over bright surfaces. The DB C006 AOD over Beijing outperformed the DT C006 AOD and produced "good fraction".

The spatial distribution of the AOD values was high over the southeastern region and low over the northwestern region. Modification of the DT C006 algorithm resulted in an increased AOD (0.0085) over this region. Although the seasonal geographical distribution exhibited similar spatial patterns as the yearly mean distribution, the AOD values were higher in spring and summer and relatively low in autumn and winter. Greater positive changes (~0.2) from DT C051 to C006 occurred in the southeastern areas during summer as a result of the updated cloud-masking. The collocated DT retrieval results

showed the same spatial distribution patterns as the other two. There was an increase frequency from DT C051 to DT C006 in the range of 0.6–1.5 over the two sites, and the AOD from DB retrievals had a very narrow range within the range from 0.1–0.3.

Both the DT and DB MODIS C006 AOD retrievals have been improved for the Beijing-Tianjin-Hebei region. These products can be applied to estimate aerosol spatial distribution variations and to evaluate the air quality in this region. The DB algorithm is recommended for Beijing and Xianghe due to its extensive applicability over land. The DT algorithm is the best for Xianghe due to the limitation in the DT algorithm over urban surfaces, i.e., sparsely vegetated surfaces.

Author Contributions: Xuejin Sun conceived and designed the experiments; Ke Wang and Yongbo Zhou analyzed the data and wrote the paper; Chuanliang Zhang proposed valuable comments for the discussion. Xuejin Sun, Yongbo Zhou revised the manuscript.

Conflicts of Interest: The authors declare no conflict of interest.

References

1. Kaufman, Y.J.; Tanre, D.; Boucher, O. A satellite view of aerosols in the climate system. *Nature* **2002**, *419*, 215–223. [CrossRef] [PubMed]
2. Koren, I.; Altaratz, O.; Remer, L.A.; Feingold, G.; Martins, J.V.; Heiblum, R.H. Aerosol-induced intensification of rain from the tropics to the mid-latitudes. *Nat. Geosci.* **2012**, *5*, 118–122. [CrossRef]
3. Cheung, H.C.; Wang, T.; Baumann, K.; Guo, H. Influence of regional pollution outflow on the concentrations of fine particulate matter and visibility in the coastal area of southern China. *Atmos. Environ.* **2005**, *39*, 6463–6474. [CrossRef]
4. Pope, C.A.; Dockery, D.W. Health effects of fine particulate air pollution: Lines that connect. *J. Air Waste Manag. Assoc.* **2006**, *56*, 709–742. [CrossRef] [PubMed]
5. Holben, B.N.; Tanre, D.; Smirnov, A.; Eck, T.F.; Slutsker, I.; Abuhassan, N.; Newcomb, W.W.; Schafer, J.S.; Chatenet, B.; Lavenu, F.; et al. An emerging ground-based aerosol climatology: Aerosol optical depth from AERONET. *J. Geophys. Res. Atmos.* **2001**, *106*, 12067–12097. [CrossRef]
6. Curier, R.L.; Veefkind, J.P.; Braak, R.; Veihelmann, B.; Torres, O.; de Leeuw, G. Retrieval of aerosol optical properties from OMI radiances using a multiwavelength algorithm: Application to western Europe. *J. Geophys. Res. Atmos.* **2008**, *113*. [CrossRef]
7. Hauser, A.; Oesch, D.; Foppa, N.; Wunderle, S. NOAA AVHRR derived aerosol optical depth over land. *J. Geophys. Res. Atmos.* **2005**, *110*. [CrossRef]
8. Kittaka, C.; Winker, D.M.; Vaughan, M.A.; Omar, A.; Remer, L.A. Intercomparison of column aerosol optical depths from CALIPSO and MODIS-Aqua. *Atmos. Meas. Tech.* **2011**, *4*, 131–141. [CrossRef]
9. Remer, L.A.; Kaufman, Y.J.; Tanre, D.; Mattoo, S.; Chu, D.A.; Martins, J.V.; Li, R.R.; Ichoku, C.; Levy, R.C.; Kleidman, R.G.; et al. The MODIS aerosol algorithm, products, and validation. *J. Atmos. Sci.* **2005**, *62*, 947–973. [CrossRef]
10. Torres, O.; Bhartia, P.K.; Herman, J.R.; Sinyuk, A.; Ginoux, P.; Holben, B. A long-term record of aerosol optical depth from TOMS observations and comparison to AERONET measurements. *J. Atmos. Sci.* **2002**, *59*, 398–413. [CrossRef]
11. Zhou, C.Y.; Liu, Q.H.; Zhong, B.; Sun, L.; Xin, X.Z. Retrieval of Aerosol Optical Thickness from Hj-1a/B Images Using Structure Function Method. In Proceedings of the 2009 IEEE International Geoscience and Remote Sensing Symposium, Cape Town, South Africa, 12–17 July 2009; pp. 413–416.
12. Levy, R.C.; Mattoo, S.; Munchak, L.A.; Remer, L.A.; Sayer, A.M.; Patadia, F.; Hsu, N.C. The Collection 6 MODIS aerosol products over land and ocean. *Atmos. Meas. Tech.* **2013**, *6*, 2989–3034. [CrossRef]
13. Kaufman, Y.J.; Tanre, D.; Remer, L.A.; Vermote, E.F.; Chu, A.; Holben, B.N. Operational remote sensing of tropospheric aerosol over land from EOS moderate resolution imaging spectroradiometer. *J. Geophys. Res. Atmos.* **1997**, *102*, 17051–17067. [CrossRef]

14. Holben, B.N.; Eck, T.F.; Slutsker, I.; Tanre, D.; Buis, J.P.; Setzer, A.; Vermote, E.; Reagan, J.A.; Kaufman, Y.J.; Nakajima, T.; et al. AERONET-A federated instrument network and data archive for aerosol characterization. *Remote Sens. Environ.* **1998**, *66*, 1–16. [CrossRef]

15. Levy, R.C.; Remer, L.A.; Kleidman, R.G.; Mattoo, S.; Ichoku, C.; Kahn, R.; Eck, T.F. Global evaluation of the Collection 5 MODIS dark-target aerosol products over land. *Atmos. Chem. Phys.* **2010**, *10*, 10399–10420. [CrossRef]

16. Milinevsky, G.; Danylevsky, V.; Bovchaliuk, V.; Bovchaliuk, A.; Goloub, P.; Dubovik, O.; Kabashnikov, V.; Chaikovsky, A.; Miatselskaya, N.; Mishchenko, M.; et al. Aerosol seasonal variations over urban-industrial regions in Ukraine according to AERONET and POLDER measurements. *Atmos. Meas. Tech.* **2014**, *7*, 1459–1474. [CrossRef]

17. Papadimas, C.D.; Hatzianastassiou, N.; Mihalopoulos, N.; Kanakidou, M.; Katsoulis, B.D.; Vardavas, I. Assessment of the MODIS Collections C005 and C004 aerosol optical depth products over the Mediterranean basin. *Atmos. Chem. Phys.* **2009**, *9*, 2987–2999. [CrossRef]

18. Li, B.; Yuan, H.; Feng, N.; Tao, S. Comparing MODIS and AERONET aerosol optical depth over China. *J. Remote Sens.* **2009**, *30*, 6519–6529. [CrossRef]

19. Floutsi, A.A.; Korras-Carraca, M.B.; Matsoukas, C.; Hatzianastassiou, N.; Biskos, G. Climatology and trends of aerosol optical depth over the Mediterranean basin during the last 12 years (2002–2014) based on Collection 006 MODIS–Aqua data. *Sci. Total Environ.* **2016**, *551*, 292–303. [CrossRef] [PubMed]

20. Bilal, M.; Nichol, J.E.; Nazeer, M. Validation of Aqua-MODIS C051 and C006 Operational Aerosol Products Using AERONET Measurements Over Pakistan. *IEEE J. Sel. Top. Appl. Earth Obs. Remote Sens.* **2016**, *9*, 2074–2080. [CrossRef]

21. Cai, W.; Li, K.; Liao, H.; Wang, H.; Wu, L. Weather conditions conducive to Beijing severe haze more frequent under climate change. *Nat. Clim. Chang.* **2017**, *7*, 257. [CrossRef]

22. Bilal, M.; Nichol, J.E. Evaluation of MODIS aerosol retrieval algorithms over the Beijing-Tianjin-Hebei region during low to very high pollution events. *J. Geophys. Res. Atmos.* **2015**, *120*, 7941–7957. [CrossRef]

23. Chen, W.; Fan, A.; Yan, L. Performance of MODIS C6 Aerosol Product during Frequent Haze-Fog Events: A Case Study of Beijing. *Remote Sens.* **2017**, *9*. [CrossRef]

24. Sun, L.; Li, R.; Tian, X.; Wei, J. Analysis of the Temporal and Spatial Variation of Aerosols in the Beijing-Tianjin-Hebei Region with a 1 km AOD Product. *Aerosol Air Qual. Res.* **2017**, *17*, 923–935. [CrossRef]

25. Bilal, M.; Nichol, J.E.; Chan, P.W. Validation and accuracy assessment of a Simplified Aerosol Retrieval Algorithm (SARA) over Beijing under low and high aerosol loadings and dust storms. *Remote Sens. Environ.* **2014**, *153*, 50–60. [CrossRef]

26. Wei, J.; Sun, L. Comparison and Evaluation of Different MODIS Aerosol Optical Depth Products over the Beijing-Tianjin-Hebei Region in China. *IEEE J. Sel. Top. Appl. Earth Obs. Remote Sens.* **2017**, *10*, 835–844. [CrossRef]

27. Levy, R.C.; Leptoukh, G.G.; Kahn, R.; Zubko, V.; Gopalan, A.; Remer, L.A. A Critical Look at Deriving Monthly Aerosol Optical Depth from Satellite Data. *IEEE Trans. Geosci. Remote* **2009**, *47*, 2942–2956. [CrossRef]

28. Hsu, N.C.; Tsay, S.C.; King, M.D.; Herman, J.R. Aerosol properties over bright-reflecting source regions. *IEEE Trans. Geosci. Remote* **2004**, *42*, 557–569. [CrossRef]

29. Hsu, N.C.; Jeong, M.J.; Bettenhausen, C.; Sayer, A.M.; Hansell, R.; Seftor, C.S.; Huang, J.; Tsay, S.C. Enhanced Deep Blue aerosol retrieval algorithm: The second generation. *J. Geophys. Res. Atmos.* **2013**, *118*, 9296–9315. [CrossRef]

30. Lyapustin, A.; Wang, Y.; Xiong, X.; Meister, G.; Platnick, S.; Levy, R.; Franz, B.; Korkin, S.; Hilker, T.; Tucker, J.; et al. Scientific impact of MODIS C5 calibration degradation and C6+ improvements. *Atmos. Meas. Tech.* **2014**, *7*, 4353–4365. [CrossRef]

31. Ichoku, C.; Chu, D.A.; Mattoo, S.; Kaufman, Y.J.; Remer, L.A.; Tanre, D.; Slutsker, I.; Holben, B.N. A spatio-temporal approach for global validation and analysis of MODIS aerosol products. *Geophys. Res. Lett.* **2002**, *29*. [CrossRef]

32. Petrenko, M.; Ichoku, C.; Leptoukh, G. Multi-sensor Aerosol Products Sampling System (MAPSS). *Atmos. Meas. Tech.* **2012**, *5*, 913–926. [CrossRef]

33. Mishchenko, M.I.; Cairns, B.; Hansen, J.E.; Travis, L.D.; Burg, R.; Kaufman, Y.J.; Martins, J.V.; Shettle, E.P. Monitoring of aerosol forcing of climate from space: Analysis of measurement requirements. *J. Quant. Spectrosc. Radiat. Transf.* **2004**, *88*, 149–161. [CrossRef]

34. Hansen, J.; Rossow, W.; Carlson, B.; Lacis, A.; Travis, L.; Delgenio, A.; Fung, I.; Cairns, B.; Mishchenko, M.; Sato, M. Low-cost long-term monitoring of global climate forgings and feedbacks. *Clim. Chang.* **1995**, *31*, 247–271. [CrossRef]

35. Tao, M.; Chen, L.; Wang, Z.; Tao, J.; Che, H.; Wang, X.; Wang, Y. Comparison and evaluation of the MODIS Collection 6 aerosol data in China. *J. Geophys. Res. Atmos.* **2015**, *120*, 6992–7005. [CrossRef]

36. Sayer, A.M.; Hsu, N.C.; Bettenhausen, C.; Jeong, M.J. Validation and uncertainty estimates for MODIS Collection 6 "Deep Blue" aerosol data. *J. Geophys. Res. Atmos.* **2013**, *118*, 7864–7872. [CrossRef]

37. He, Q.; Zhang, M.; Huang, B.; Tong, X. MODIS 3 km and 10 km aerosol optical depth for China: Evaluation and comparison. *Atmos. Environ.* **2017**, *153*, 150–162. [CrossRef]

38. Wang, L.; Xin, J.; Li, X.; Wang, Y. The variability of biomass burning and its influence on regional aerosol properties during the wheat harvest season in North China. *Atmos. Res.* **2015**, *157*, 153–163. [CrossRef]

39. Remer, L.A.; Mattoo, S.; Levy, R.C.; Munchak, L.A. MODIS 3 km aerosol product: Algorithm and global perspective. *Atmos. Meas. Tech.* **2013**, *6*, 1829–1844. [CrossRef]

40. Liu, H.; Tang, X.M.; Cao, W.; Xie, Z.Y.; Lei, J.H.; Li, M.; Gao, Y. Spatio-Temporal Variations of Aerosol Optical Depth over Areas Around Beijing in Recent 14 Years. *Adv. Mater. Res.* **2014**, *997*, 843–846. [CrossRef]

41. Twomey, S.; Squires, P. The Influence of Cloud Nucleus Population on the Microstructure and Stability of Convective Clouds. *Tellus* **1959**, *11*, 408–411. [CrossRef]